Cost-benefit Tradeoff Mediates the Rule- to Memory-based Transition during Practice

Guochun Yang[1,2,*] and Jiefeng Jiang[1,2,3,*]

[1] Cognitive Control Collaborative, University of Iowa, Iowa City, IA 52242, USA.
[2] Department of Psychological and Brain Sciences, University of Iowa, Iowa City, IA 52242, USA.
[3] Iowa Neuroscience Institute, University of Iowa, Iowa City, IA 52242, USA.
*Correspondence: guochun-yang@uiowa.edu (G.Y.) and jiefeng-jiang@uiowa.edu (J.J.)

Abstract

Practice not only improves task performance, but also changes task execution from rule- to memory-based processing by incorporating experiences from practice. We tested the hypothesis that strategy transition in task learning results from a cost-benefit analysis of candidate strategies. Participants learned two task sequences and were then queried the task type at a cued sequence and position. Behavioral improvement with practice can be accounted for by a computational model implementing cost-benefit analysis. Model-guided fMRI analysis shows frontal and parietal activations scaling with the demand of executing rule and memory strategy, respectively. fMRI activation pattern analysis further reveals widespread strategy-specific neural representations when their corresponding strategy is executed. Lastly, strategy transition is related to neural representation change in the dorsolateral prefrontal cortex and pattern separation in the ventromedial prefrontal cortex and the hippocampus. These findings shed light on how practice optimizes task performance by shifting task representations at the strategy level.

Keywords: cost-benefit tradeoff; practice; task representation; cognitive control; replay; memory retrieval; pattern separation

Introduction

"Practice makes perfect". During task learning, practice improves performance and reduces effort. Practice effects occur in multiple cognitive functions supporting task execution. For example, it speeds up processing of task-relevant information,[1,2]. Additionally, with practice task execution becomes more robust to distraction and requires less attentional control.[3,4] Crucially, practice also changes how task is performed. For example, novice chess players must apply the rules to search for the best move, whereas experienced players can leverage their memory of previous games to recognize the board configuration to reduce the effort of search and retrieve the best move.[5-7] This transition from rule-based processing to memory-based retrieval is termed automatization and is vital in learning complex tasks (e.g., chess, programming and arithmetic).[8]

Rule- and memory-based processing are commonly recognized in theoretical frameworks of cognition.[9] According to the Evans et al.'s[10,11] dual-processing theories, the brain operates with two distinct reasoning subsystems: one characterized by automatic, associative and intuitive processes, and the other marked by controlled, rule-based and effortful processes. These two different systems are supposed to be driven by different neural systems.[10,11] Kahneman[12] also proposed a similar dichotomy between fast and slow thinking systems in the decision-making processes. However, in the context of task learning, it is less known how the brain shifts from rule-based to memory-based processing with practice.

We hypothesize that the transition from rule- to memory-based processing can be explained by cost-benefit analysis similar to theories of goal-directed behavior.[13,14] Specifically, whether to engage rule- or memory-based processing is hypothesized as a decision driven by balancing achieving the goal (benefit) and reducing effort (cost). Consistent with this view, Schuck et al.[15] observed that participants spontaneously shift from a rule-based strategy to a less effortful strategy relying on task-irrelevant information. Conceptually, memory-based strategy retrieves the answer directly and bypasses execution of the rules. Thus it is less effortful/costly than rule-based processing. On the other hand, memory-based strategy depends on accumulation of experience. Thus, its benefit starts off low and gradually increases with practice, whereas the benefit of rule-based processing remains consistently high from the outset. Therefore, early in task learning (e.g., a novice chess player), rule-based processing is favored because its higher benefit outweighs its higher cost than memory-based processing. As more experience is gained (e.g., a veteran chess player), the increased benefit makes memory-based processing outperform rule-based processing in cost-benefit tradeoff, leading to a strategy transition from rule- to memory-based processing.

To test this hypothesis, we designed a two-phase experiment. Human participants (n = 33) learned two task sequences in the training phase (Fig. 1A; each task sequence consists of five distinct delayed matching tasks, see Materials and Methods). In the following test phase, participants were asked to report the task type at a cued position from one sequence (e.g., A4, denoting the 4th position in sequence A) while

undergoing fMRI scanning (Fig. 1B). As detailed above, we expected that participants started with rule-based processing (i.e., by replaying the task sequence to identify the cued task) and switched to memory-based processing when the cue-task associations become available with practice (Fig. 1C). Based on the cost-benefit analysis, we constructed a computational model to estimate the time of transition based on behavioral data. Model-based univariate fMRI analysis revealed distinct brain regions reflecting replay and memory strategies, and multivariate analysis identified widespread double dissociation showing that fMRI activation patterns on replay and memory trials are more consistent with their respective strategy than the other. Additionally, the computational model estimated transition points that served as an event boundary[16-19] to separates task learning into two segments (i.e., replay- and memory-based). To identify neural underpinnings associated with the transition, we tested how neural representations differ between pre- and post-transition trials and found that fMRI activation patterns in the right dorsolateral prefrontal cortex (dlPFC) exhibit a boundary effect, such that trials on the same side of the transition point show more similar activation patterns than those crossing the transition point. Lastly, the hypothesis predicted that the cue-task association strengthens over time. One way to

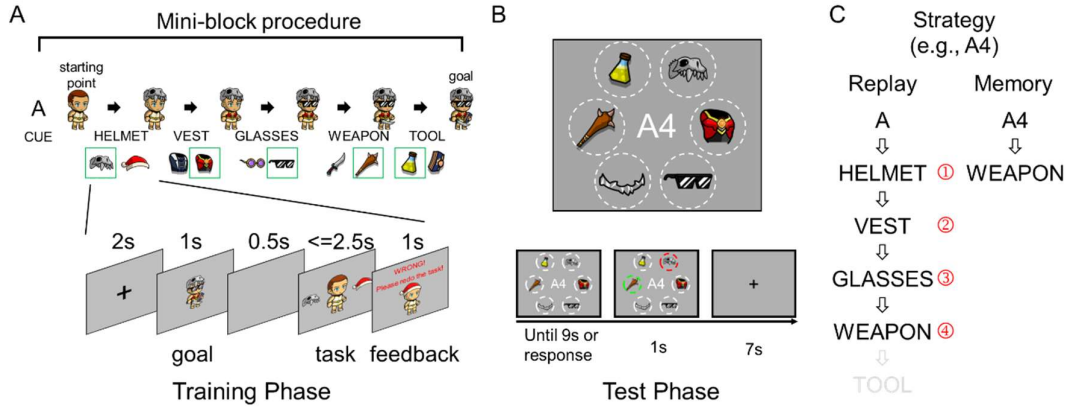

Fig. 1. Experimental design. A) Training phase design. Top panel: During the training phase, participants learned two sequences of tasks (one example sequence shown) with practice. Each sequence consists of five different tasks in a fixed order, indicated by a cue (A or B) presented before the first trial of the corresponding sequence. Each task requires the participant to equip an avatar with a specific type of gear (e.g., helmet). Bottom panel: A task starts with a goal image and then two option gears, one on each side of an avatar. Participants are required to choose the gear that matches the goal image. The goal image was randomized for each mini-block to ensure that the sequences are defined by equipment types (e.g., weapon) rather than specific stimuli (e.g., dagger). B) Test phase design. Top panel: During the test phase, a cue denoting the position from a sequence (e.g., A4, denoting the 4th position in sequence A) is displayed in the center of the screen. Participants are required to identify the task type at the cued position of the sequence by selecting the equipment representing the task type (e.g., nunchaku, representing the weapon task). Bottom panel: trial time course. C) Illustration of the two strategies. The replay strategy would recall the cued sequence (e.g., A) and replay from the first position till the cued position (e.g., 4), and the memory strategy would retrieve the association between the cue (e.g., A4) and the task (e.g., weapon) directly.

strength the associations is to reduce their interference by making their neural representations more distinct, a neurocomputation termed pattern separation.[20] In task learning, pattern separation has been observed in the hippocampus and the neocortex.[21] This prediction was supported by the finding that pattern separation of cue-task associations increased over time in the left hippocampus and the ventromedial PFC (vmPFC).

Results

Model-free behavioral results

In the training phase, participants were trained until they accurately (with accuracy > 90%) remembered transitions between tasks (see Methods). For test phase data, we first conducted model-free analysis. Trial-wise response times (RTs) and error rates (ERs) were analyzed separately using linear mixed effect (LME) models. Predictors included cued position (1–4), block (1–6) and their interaction. RT results (Fig. 2A) showed a significant main effect of block (β = –0.30, SE = 0.03, 95% confidence interval (CI) = [–0.36 –0.25], $t(34.1) = -11.27$, $p < .001$, $\eta_p^2 = .38$), a significant main effect of position (β = 0.45, SE = 0.04, 95% CI = [0.36 0.54], $t(34.0) = 10.02$, $p < .001$, $\eta_p^2 = .57$), and a significant interaction effect (β = –0.10, SE = 0.02, 95% CI = [–0.13 –0.07], $t(70.5) = -6.27$, $p < .001$, $\eta_p^2 = .06$). Post-hoc comparisons showed that the linear effect of position in block 1/2 was larger than block 2−6/4−6, respectively (ps < .05). ER results showed a significant main effect of block (β = –0.19, SE = 0.04, 95% CI = [–0.27 –0.10], $t(34.0) = -4.22$, $p < .001$, $\eta_p^2 = .05$), position (β = 0.21, SE = 0.04, 95% CI = [0.12 0.29], $t(37.6) = 4.67$, $p < .001$, $\eta_p^2 = .06$), and a significant interaction effect (β = –0.12, SE = 0.04, 95% CI = [–0.20 –0.04], $t(44.3) = -3.12$, $p = .003$, $\eta_p^2 = .02$). Post-hoc comparisons suggested that the linear effect of position in block 1 was larger than block 3 and 6, and that this effect in block 2 was larger than block 3−6, ps < .05. We also replicated these findings using all five cued positions (Supplementary Note S1). Overall, we observed three patterns: (1) performance, when collapsed across cued positions, improved over time; (2) performance, when collapsed across blocks, was worse when later position was cued; and (3) the negative association between performance and cued position decreased with time.

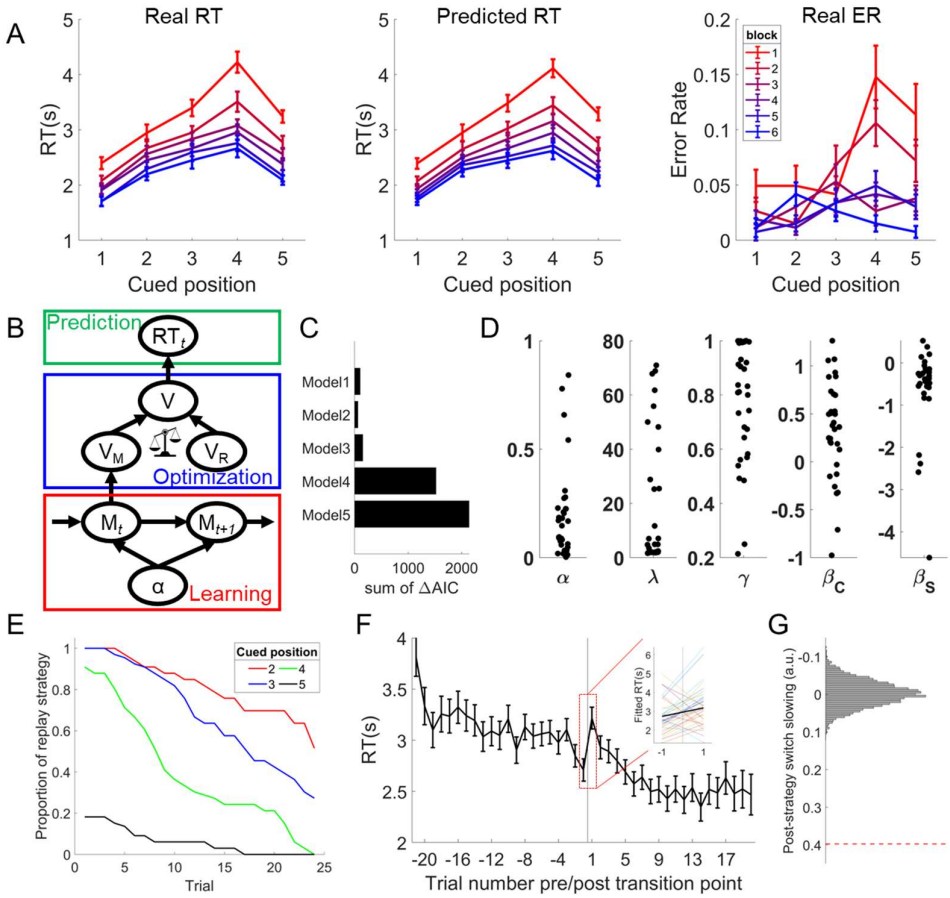

Figure 2. Behavioral and computational modeling results. A) behavioral data (RT, left panel, and ER, right panel) and model predicted RT (middle panel) displayed as a function of cued position and block. Error bars denote standard errors of mean (SEMs). B) The structure of the generative model. It includes three main components: learning, optimization and prediction. The learning component updates the memory strength of the cue-task associations (i.e., a probabilistic distribution of the correct task, denoted as M) using a delta rule with learning rate α. The optimization component makes winner-take-all decisions of which strategy to apply using cost-benefit analyses. The prediction component predicts trial-wise RT based on linear predictors of values driven by replay cost (V_R) or memory strength (V_M), depending on the strategy used. The model was fit to trial-wise RT data to estimate model parameters and trial-wise prediction of the strategy used. C) Model comparison based on the group-level ΔAIC (Akaike information criteria), i.e., increased AIC of alternative models (see Table 1 and Methods) compared to the winning model (Model0, illustrated in panel B). D) Individual model-estimated parameters (α = learning rate, λ = cost-benefit tradeoff, γ = recency effect, see definition in Materials and Methods) and beta coefficients for replay cost (C) and memory strength (S) effects. E) Change of model predicted strategy over time. The Y axis shows the model-inferred proportion of participants using the replay strategy. Trials were counted for each cue separately. F) The RT as a function of trial number relative to the cue's transition point. The inset highlights the increase of RT on the trial following estimated strategy switch. Error bars denote SEMs. G) Post-strategy switch slowing of real data (dashed red line) and its null distribution (histogram) estimated using randomly selected transition points.

Model-based behavioral results

We constructed a computational model to capture the dynamics of transitioning from replay to memory strategy (i.e., the processing type used, see Fig. 2B and Materials and Methods). On each trial, the model performs a cost-benefit analysis to determine which strategy to use based on their values, defined as a weighted sum of cost and benefit. Conceptually, the replay strategy retrieves a task before the cued position (e.g., the first task of a sequence) and replays later tasks using sequential memory until the cued position is reached. On the other hand, the memory strategy directly retrieves the cued task through cue-task associations. Thus, the replay strategy is more effortful (and thus costly) than the memory strategy. Early in the test phase, the cue-task association is weak, whereas the participants had strong sequential memory of the task order from the training phase. Thus, the replay strategy provides better value than memory strategy due to its higher benefit (despite of higher cost) and is favored. As participants received feedback with practice, the cue-task association became stronger. Along with its less effort than replay, the memory strategy eventually achieved better cost-benefit tradeoff, leading to the transition of strategy.

Based on trial-wise model prediction of which strategy to use, trials were categorized as replay and memory trials. For each participant, the model outputs were then linked to trial-wise RT using a linear model (Model0, Table 1) with the following regressors: (1) replay cost (C, number of steps from replay start to cued position) for replay trials, (2) the strength of the cue-task association (S) for memory trials quantified as the reversed entropy of the task distribution conditioned on the cued position, (3) trial type (i.e., replay ($Type_R$) vs. memory ($Type_M$)), (4) the interaction between C and aggregated number of replayed steps since the beginning of experiment ($C*Times_R$) that reflects the practice effect of replay (i.e., more experience would accelerate replay and reduce the effect of C on RT), (5) log-transformed trial number that reflects practice effect not involving strategy switch and (6) response (dummy coded). We compared Model0 to its reduced versions (Table 1) using likelihood ratio test at the group level. Comparison between unnested models was achieved through Akaike information criteria (AIC). Model0 outperformed all other models (ps < 0.001, Fig. 2C). Of note, the two reduced models that assume either replay strategy only (Model4, with only C) or neither of replay nor memory strategy (Model5, without C or S) were outperformed by all other models that assumes two strategies (ps < .001), suggesting that both strategies were used. In addition, to test whether the mentally estimated cost of replay strategy discounts with more replayed experience, as indicated by the interaction effect of $C*Times_R$, we compared M0 to a new model (M6, supplementary Note S2). The results suggested no evidence of such a discount.

Individual model parameters are shown in Fig. 2D. The effect of C was significantly above 0 (β = 0.33, SE = 0.09, Cohen's d = 0.64, 95% CI = [0.15 0.51], $t(32) = 3.70$, $p < .001$), indicating that participants were slower when the model predicted more steps to replay. The interaction between the simulation cost and the

accumulated replay trials was significant (β = –0.09, SE = 0.04, Cohen's d = –0.38, 95% CI = [–0.18 –0.01], $t(32)$ = –2.20, p = .035), suggesting that replay accelerated over time. The memory strength effect (S) was also significant (β = –0.61, SE = 0.17, Cohen's d = –0.61, 95% CI = [–0.96 –0.26], $t(32)$ = –3.52, p = .001), suggesting that participants responded faster when the model predicts a stronger cue-task association on memory trials. Other than the cost-benefit analysis, one alternative hypothesis was that the strategy to use was solely based on the utility of the memory strategy (i.e., strategy switches once cue-task association is strong enough regardless of the value of the replay strategy). This would predict ceiling values (i.e., 100, as per our definition) for λ in cost-benefit analysis (Eq. 4). Contrary to this prediction, none of the subjects reached the ceiling value. Instead, we observed a distribution of λ ranging from 1.6 to 70.9 (Fig. 2D), suggesting a comparison between memory and replay strategies.

Model-predicted proportion of participants using replay strategy decreased over time (Fig. 2E), indicating that the replay strategy was replaced by the memory strategy with practice. We defined transition points as immediately before the trial on which the value of the memory strategy first surpassed the replay strategy (Fig. S1A). Transition points were defined for each cue except for cues at position 1, because no replay is necessary. Among the remaining 192 trials for cued positions 2–5, the model predicted that a participant applied the replay strategy on 94 ± 37 trials, varying from 21 to 166 trials.

Table 1. Description of tested models and corresponding model comparison results.

Model regressors	M0*	M1	M2	M3	M4	M5
Log(Trial)	+	+	+	+	+	+
Response	+	+	+	+	+	+
C	+	+	+	+	+	–
S	+	+	+	+	–	–
$Type_R$ / $Type_M$	+	–	+	–	–	–
C_R*$Times_R$	+	+	–	–	+	–
AIC	–4019	–3917	–3959	–3866	–2497	–1878
Likelihood ratio test with M0 (p value)		< .001	< .001	< .001	< .001	< .001

Note. C = replay cost; S = memory strength; R = replay trial; M = memory trial; AIC = Akaike information criteria. * denotes the winning model.

Behavioral slowing following model-predicted strategy transition

To validate the transition points predicted by the model, we tested the strategy switch cost following the transition point.[22] Using an LME model, we observed a significant increase of RT after transition points (β = 0.40, SE = 0.15, 95% CI = [0.10 0.69], $t(80.5)$ = 2.64, p = .0010, η_p^2 = .15, Fig. 2F). To examine whether this effect is linked to the model-predicted transition points, we repeated this analysis for 5,000 times using randomly selected transition points for each cue and each subject. The observed post-switch slowing is stronger than all random ones (p < .001, Fig. 2G). It

is noteworthy that this effect is independent from the model fitting, which only assumes the main RT for memory and replay trials can be different (i.e., different intercepts), without any assumption for the two adjacent trials of the transition point. We further tested the alternative explanation that the structure of the computational model is biased to reporting artificial post transition slowing. To this end, we repeated the post-transition slowing analysis using randomly sampled model parameters while keeping the architecture of the model constant for 5,000 times. The median of the resulting distribution was centered around 0 and significantly lower than the observed post-switch slowing (Fig. S1B), thus ruling out the possibility that the model artificially introduced a post-switch slowing effect.

Frontoparietal fMRI activation for replay and memory strategies

We validated our fMRI data using univariate analyses conducted on single-trial activation maps. We predicted stronger fMRI activation when more steps are replayed on replay trials.[23] On memory trials, fMRI activation may be stronger when the cue-task association is stronger (reflecting memory retrieval effect)[24] or weaker (reflecting uncertainty effect)[25]. We conducted an LME model analysis for replay and memory trials separately. For replay trials, higher replay cost was accompanied by stronger activation in several frontal regions, including Human Connectome Project (HCP) Atlas[26] areas 8C, anterior inferior frontal junction (IFJa), posterior 47 rostral (p47r), anterior 47 rostral (a47r), anterior 9-46 ventral (a9-46v), posterior 32 prime (p32pr), inferior 6-8 (i6-8) in left hemisphere and 8C, posterior 9-46 ventral (p9-46v), 44 in right hemisphere, ps < 0.05 corrected (Fig. 3A-B). For memory trials, we found stronger brain activation with stronger memory of the cued position-task association in the left PF (Fig. 3C-D, $p < 0.05$ corrected), and stronger brain activation with weaker memory of the cued position-task association in the left supplementary and cingulate eye field (SCEF) and left posterior IFJ (IFJp) (Fig. 3E-F). No other regions survived the correction for multiple comparisons. These results are consistent with previous findings[25,27,28] and provide a sanity check of the fMRI data. In addition, we also found a weak increase of activities after the transition point mainly in frontal regions (Fig. S2), which was in line with the behavioral finding of strategy transition cost (Fig. 2F-G).

Given the importance of the hippocampus in memory[29] and replay,[30] we tested the effects on bilateral hippocampus as a priori ROIs. Results suggest that the bilateral hippocampus showed no enhanced activity with increased simulation cost (left hippocampus: $\beta = -0.0004$, SE = 0.0061, 95% CI = [–0.0123 0.0115], $t(32.1) = -0.07$, $p = .528$ uncorrected, $\eta_p^2 = .0000$; right hippocampus: $\beta = -0.0051$, SE = 0.0070, 95% CI = [–0.0189 0.0087], $t(30.5) = -0.73$, $p = .764$ uncorrected, $\eta_p^2 = .0004$). In addition, they showed no amplified activity in response to stronger memory association (left hippocampus: $\beta = -0.0077$, SE = 0.0087, 95% CI = [–0.0247 0.0093], $t(43.1) = -0.89$, $p = .813$ uncorrected, $\eta_p^2 = .0010$; right hippocampus: $\beta = -0.0141$, SE = 0.0099, 95% CI = [–0.0336 0.0054], $t(526.3) = -1.42$, $p = .922$ uncorrected, $\eta_p^2 = .0026$). Furthermore, there was no observed increase in activity following the

transition (left hippocampus: β = 0.0110, SE = 0.0662, 95% CI = [–0.1194 0.1414], t(258.1) = 0.17, p = .434 uncorrected, η_p^2 = .0002; right hippocampus: β = 0.0147, SE = 0.0696, 95% CI = [–0.0223 0.1517], t(30.9) = 0.21, p = .417 uncorrected, η_p^2 = .0003). These results suggest that the univariate activation in bilateral hippocampus did not reflect replay and memory in our study.

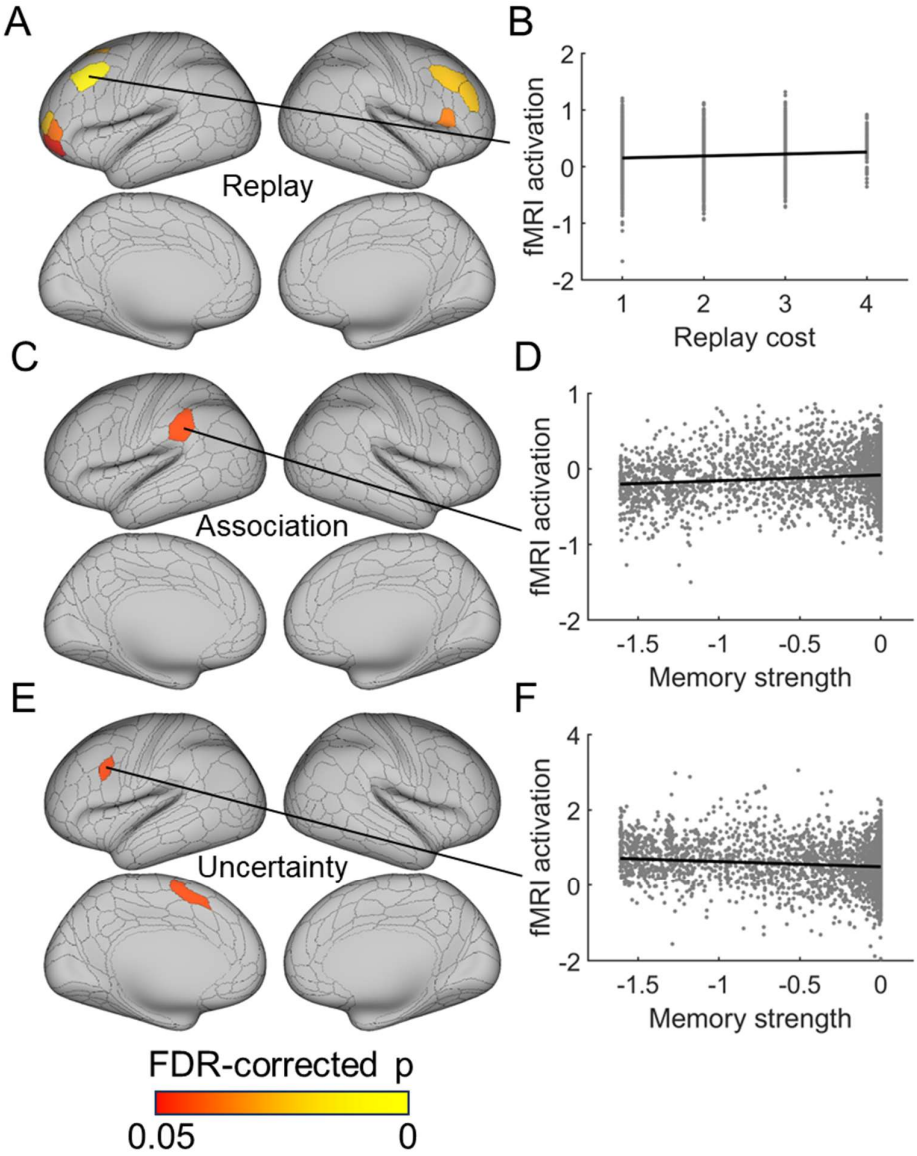

Figure 3. Frontoparietal fMRI activation for replay and memory strategies. A) Regions showing higher fMRI activation with higher replay cost (i.e., number of steps replayed). B) Trial-wise fMRI activation in the left 8C region as a function of replay cost. C) and E) are regions showing higher trial-wise activation for stronger memory strength (i.e., cue-task associations), and higher trial-wise activation for lower memory strength (i.e., higher uncertainty), respectively. D) and F) show the trial-wise fMRI activation in the left PF and left IFJp, respectively, plotted as a function of memory strength quantified as reversed entropy.

fMRI activation patterns shift with strategy

We next investigated fMRI activation patterns reflecting the replay and memory representations, and whether these patterns change with the transition in behavioral strategy. For the replay strategy, we predicted that the similarity of voxel-wise activation patterns across two trials in fMRI data would reflect the number of shared replayed tasks (Fig. 4AB). For the memory strategy, we tested the cue effect such that two trials' activation patterns will be more similar if they share the same cue than not, as the cue and its association with the task are used in the memory strategy (Fig. 4AC). We expected to observe a stronger replay effect on replay than memory trials, and a stronger cue effect on memory than replay trials.

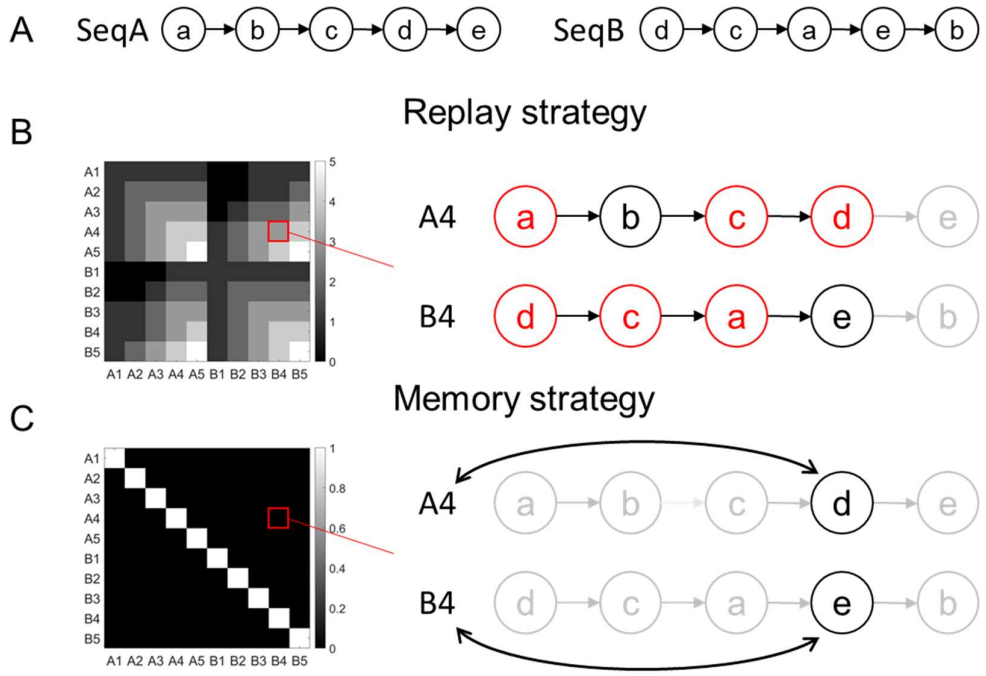

Figure 4. Coding schemes of representational similarity for replay and cue effects. A) The two task sequences. Letters a-e represent the five tasks. B) The hypothetical representational similarity for replay effect is quantified as the number of shared replayed tasks between two trials. For example, cue A4 and B4 share three tasks in replay, namely a, c and d (red nodes), resulting in a similarity level of 3. C) The hypothetical representational similarity for the cue effect (reflecting memory strategy) is defined by the concordance of the cues and hence their associated tasks. For example, the cues A4 and B4 are different, thereby yielding a similarity value of 0. The light gray nodes and arrows in panel B and C indicate the tasks that are neither replayed nor retrieved.

Results showed more widespread brain regions with replay effect on replay trials than memory trials (Fig. 5A-B) and the opposite pattern for the cue effect (Fig. 5D-E). To statistically test the strength of each effect across trial type while controlling for processing shared by both strategies (e.g., visual processing), we compared each effect between replay and memory trials. A stronger replay effect on replay trials compared to memory trials was observed in the striatum, frontoparietal, temporal and

occipital regions (Fig. 5C, *p*s < 0.05 corrected), whereas a stronger cue effect on memory than replay trials was found in similar regions with less spatial extent (Fig. 5F, *p*s < 0.05 corrected). No regions showed statistically significant effect in the opposite direction in either test. Finally, to test the double dissociation of stronger replay/cue effect on replay/memory trials, we conducted a strategy × trial type interaction analysis. We further filtered the FDR-corrected findings by requiring statistically significant ($p < 0.05$ uncorrected) stronger replay/cue effect on replay/memory trials than other trials, respectively. The double dissociation pattern was observed in bilateral frontoparietal, temporal, occipital and subcortical regions (Fig. 5G-H, see Table S1 for a detailed list of brain regions and statistics).

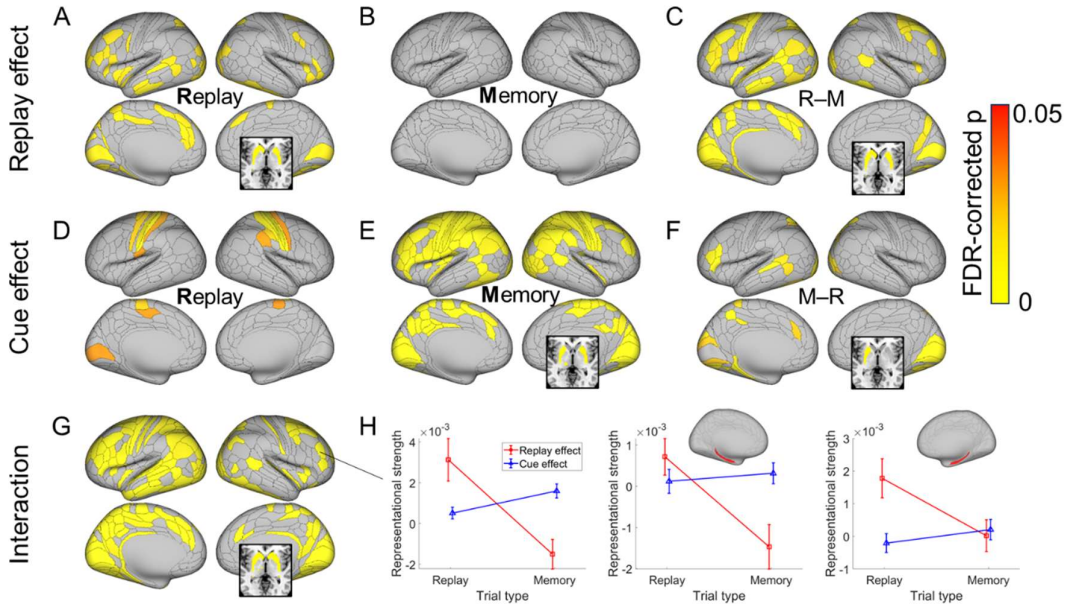

Figure 5. Double dissociation of replay and memory representations on their respective trials revealed by multivariate activation patterns. Significant representation of replay effect is observed on replay (R) trials (panel A) but not on memory (M) trials (panel B). C) A stronger replay effect on replay than memory trials (R–M) was found in frontoparietal, temporal, occipital and subcortical regions. In contrast, the cue effect exhibits in more regions on memory trials (panel E) than replay trials (panel D), and regions showing stronger memory effect on memory than replay trials (M–R) include frontoparietal, temporal, occipital and subcortical regions (panel F). G) Regions showing double dissociation (i.e., the strategy × trial type interaction) with both stronger replay effect representation in replay trials and stronger cue effect representation in memory trials. All subcortical regions are depicted in an axial slice at z = 0. H) Strength of replay and cue effects (group mean and SEM) in example regions (from left to right: the right posterior 9-46v, left hippocampus and right hippocampus), plotted as a function of trial type.

The bilateral hippocampus (Fig. H, middle and right panels) showed a stronger representation of replay effect in replay trials (left hippocampus: $t(42.7) = 3.12$, $p = .003$ uncorrected, $\eta_p^2 = .1855$; right hippocampus: $t(42.8) = 2.28$, $p = .028$ uncorrected, $\eta_p^2 = .1086$) and an interaction effect (left hippocampus: $t(175.6) = 2.78$, $p = .007$ uncorrected, $\eta_p^2 = .0929$; right hippocampus: $t(76.2) = 2.31$, $p = .023$

uncorrected, $\eta_p^2 = .0656$), but no stronger representation of cue effect in memory trials (left hippocampus: $t(144.7) = 0.50$, $p = .617$ uncorrected, $\eta_p^2 = .0056$; right hippocampus: $t(52.1) = 0.97$, $p = .337$ uncorrected, $\eta_p^2 = .0177$). This suggest that the bilateral hippocampus specifically encodes the representation of replay.

Dorsolateral PFC encodes boundary effect across the transition point

Our behavioral and modeling results suggest an abrupt shift of strategies when the value of memory retrieval outweighs the rule-based replay (Fig. 2F and Fig. S1A). We anticipated that there might be neural mechanisms sensitive to this abrupt shift,[15,31] distinct from the overall differences observed during the constant application of the two strategies (Fig. 5). Therefore, we next aimed to identify the neural substrates supporting strategy switch. To this end, we treated a transition point as a boundary separating the two time periods using different strategies. We then tested the boundary effect (i.e., higher pattern similarity between trials at the same side of boundary than different, termed as "within boundary" and "between boundary" conditions, respectively). To focus on the effects specific to the boundary, we compared pattern similarity of the trials immediately adjacent to the transition point and other temporally close trials (i.e., between 2 and 6 trials away from the transition point). We excluded trial pairs involving different cues to prevent potential confounding effects from intrinsic differences across cues (Fig. 4C). We found that the right Dorsolateral PFC (dlPFC region, area p9-46v) showed statistically significant boundary effect (Fig. 6, $\beta = 0.0109$, SE = 0.0028, 95% CI = [0.0054 0.0165], $t(1358.0) = 3.86$, $p = .023$ corrected, $\eta_p^2 = .0116$). No other regions survived the correction for multiple comparisons. This effect was stronger than its null distribution using shuffled transition points for 5,000 times ($p = .024$, Fig. 6C), suggesting that the boundary effect is tied to the model-estimated transition points. To further rule out the possibility that this finding captured a generic trial type effect (i.e., independent of the trials' temporal distance from the transition points), we repeated the same analysis by replacing the temporally close trials with trials that were more than 6 trials away from the transition point and did not observe the boundary effect ($t(30.7) = 0.84$, $p = .203$ uncorrected). In other words, it appears that this effect only occurred on trials near strategy transition and supports the relation between dlPFC representation and strategy transition. Additionally, at an uncorrected threshold level, the left hippocampus showed a numerical trend, $\beta = 0.0043$, SE = 0.0028, 95% CI = [–0.0012 0.0097], $t(1376.2) = 1.54$, $p = .061$ uncorrected, $\eta_p^2 = .0019$; but the right hippocampus showed no such an effect, $\beta = –0.0002$, SE = 0.0031, 95% CI = [–0.0063 0.0058], $t(1380.4) = –0.07$, $p = .529$ uncorrected, $\eta_p^2 = .0000$.

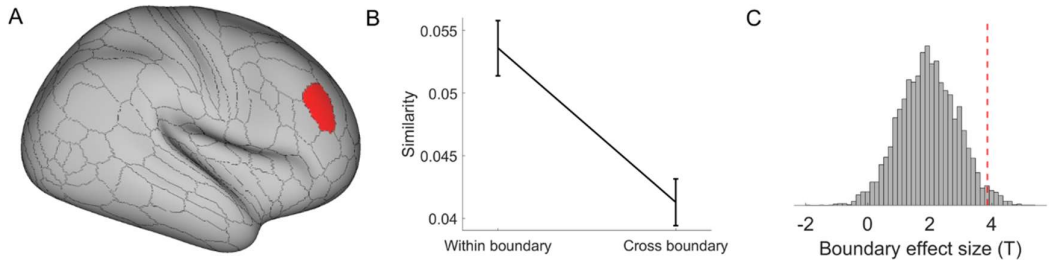

Figure 6. Dorsolateral PFC encodes boundary effect across the transition point. A) The right p9-46v shows a higher within-boundary than cross-boundary pattern similarity for trials around the transition points. B) Pattern similarity (group mean ± SEM) as a function of within/cross boundary in the region right p9-46v. C) The significant boundary effect (i.e., the higher pattern similarity in within boundary than cross boundary condition, indicated by the red dashed line), compared with a null distribution obtained by randomly shuffling the transition point for 5,000 times.

Ventromedial PFC and hippocampus pattern-separates cue-task associations

We hypothesized that the memory strategy requires the cue-task associations to be pattern separated[20] to reduce interference. As a result, pattern similarity between different cues is expected to reduce over time. To focus on strategy transition, trials were time-locked to their corresponding transition points. Trial positions containing too few (< 30) data points were excluded from the analysis. The predicted decrease of between-cue pattern similarity was observed in the left ventromedial PFC (vmPFC, 10r area, Fig. 7A, $t(52.4) = -3.93$, $p < .001$, $p = .048$ corrected, $\eta_p^2 = .2279$). No other regions survived the correction for multiple comparisons. At an uncorrected threshold level, we also found that the left hippocampus showed decreased pattern similarity between different cue-task associations over time ($t(29.2) = -1.83$, $p = .039$ uncorrected, $\eta_p^2 = .0407$ (Fig. 7B). Neither region showed a difference of pattern separation between replay and memory trials. Together, the results suggest that the vmPFC and hippocampus separate neural representations of different cue-task associations during task learning, potentially to strengthen these associative memories via reducing interference between associations.

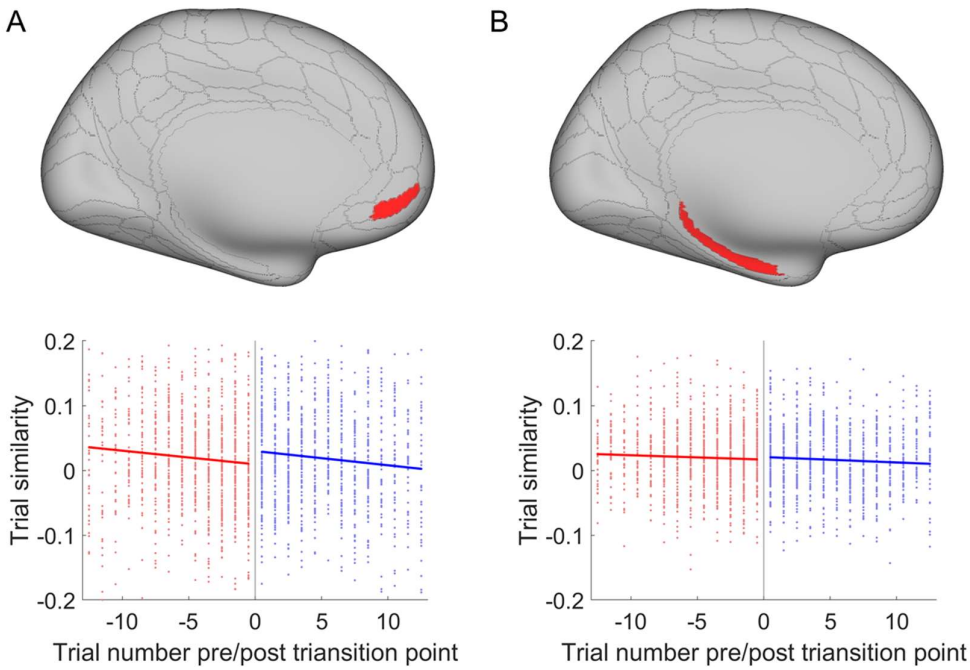

Figure 7. Ventromedial PFC and hippocampus pattern-separates cue-task associations. A) The left 10r area shows that pattern similarity among different cues decreases over time. B) The left hippocampus shows a weaker but statistically significant pattern separation. The top panels show their anatomical locations. The bottom panels show their scatter plots of trial similarity as a function of trial number relative to the transition point and the corresponding fitting lines. Red and blue colors indicate replay and memory trials, respectively.

Discussion

Practice improves task performance not only by making task execution more efficient, but also by changing the strategy in which the task is performed. Here, we investigated how task strategy and related neural representations change in task learning. After learning two task sequences, participants were asked to report the task type at a cued position from one sequence. The behavioral data show worsened performance for later cued positions, suggesting that participants adopted a strategy to replay the task sequence to obtain an answer. Additionally, the strength of the performance-cued position correlation decreases over time, which can be explained by a transition to memory-based strategy that retrieves the cued task directed from memory (i.e., performance is not sensitive to cued position). We estimated the transition point using a computational model based on cost-benefit tradeoff, in which transition occurred when the value of the memory strategy outperformed the replay strategy. Using model-guided fMRI analysis, we observed the efforts of replaying in prefrontal regions. The strength of cue-task associations was negatively associated with supplementary motor area and eye field area and positively correlated with left supramarginal gyrus. We further observed widespread double dissociation showing strategy-specific neural representations corresponding to model-predicted strategy

(Fig. 5). Related to the strategy transition, shift in neural representation is also revealed in the dlPFC (Fig. 6) and associated with a gradual pattern separation of the vmPFC and the hippocampus (Fig. 7).

Our computational model reconciles the gradual increase in pattern separation in neural data (Fig. 7, also see ref[21]) and the abrupt strategy switch (also see ref[15]) by introducing trial-level cost-benefit analysis between the two strategies. In other words, as the cue-task associations strengthen, the cost-benefit tradeoff (i.e., value) for the memory strategy increases gradually and monotonically (Fig. S1A). When it started to achieve better cost-benefit tradeoff than replay, later trials will use the memory strategy. The estimated transition points were validated by independent analyses of post-transition slowing (Fig. 2F and S1B) and the boundary effect in the dlPFC (Fig. 6). These model-based findings not only support strategy shift in practice-induced automaticity,[8] but also provides a new account to how it occurs. Specifically, model comparison results (Table 1 and Supplementary Note S2) highlight the importance of cost-benefit tradeoff in the human brain's decision-making process when choosing between alternative strategies.[13,32,33] This model also joins the increasing use of trial-level modeling approach in research of adaptive behaviors, such as flexible cognitive control[34] and strategy selection,[35] which enables fine-grained hypothesis testing on the dynamics of neural activity and behavior.

Extending previous behavioral findings showing multiple strategies in task learning,[36] our results shed light on how the rule- and memory-based processing are represented in the brain from two aspects: activation strength and representation content. The rule-based processing becomes more effortful when replaying more tasks, and this effect is associated to stronger activations in frontal regions (Fig. 3AB). The involvement of these frontal regions suggests a reliance on working memory and cognitive control, where sequences are held in mind and the answer is derived step by step.[37,38] In contrast, performance of the memory-based processing relies on strength of cue-task association, with related activations observed in left inferior parietal cortex (Fig. 3CD), highlighting the important role of this region in episodic memory retrieval.[28,39] We also observed enhanced fMRI activation with weaker memory strength in frontal eye field area and supplementary motor regions, possibly reflecting the downstream effects of uncertainty in cue-task associations on motor responses.[40] We further examined the representation content of the two strategies, which reveals a large number of brain regions showing strategy-specific fMRI activation patterns for both strategies (Fig. 4-5). This finding underscores the remarkable flexibility and adaptability of our brain in representing different processing.[41-43] This result is also in line with the fact that rule- and memory-based processing are supported by overlapping distributed brain networks. For example, in addition to the working memory and cognitive control in the rule-based processing,[3,38] the lateral prefrontal cortex also helps resolve interference and retrieval selection in memory.[44,45] Notably, the anatomically specific activation for strength and overlapping representation for content are not contradictory.[46,47] Instead, the specificity could be essential in enabling effective cost-benefit analysis among the two strategies without confusion from each other, whereas the overlapping may reflect the shared goal, and the

widespread brain involvement may reflect the necessity of brain resources allocation in such a demanding task. Overall, our results identified replay- and memory-strategy related neural representations that were selectively activated when their corresponding strategy was executed.

When focusing on behavioral and neural changes related to strategy transition, we first observed a behavioral post-transition slowing effect (Fig. 2F) and a numerical trend of increased fMRI activation in prefrontal cortex following estimated transition points (Fig. S2). We further found that dlPFC activation patterns are different before and after strategy transition (Fig. 6). This difference is specific to trials near the transition point instead of reflecting the difference between the two strategies. The boundary effect may be attributable to two non-exclusive sources. First, it may reflect neural activities preparing for transition.[15] Second, the boundary effect may signal the establishment of an event boundary[31,48] that segments experiences based on the strategy used to reduce the interference from the replay strategy after strategy transition.[30]

Pattern separation is a fundamental mechanism for organizing the memories of multiple similar items.[20] We showed that with practice, the neural pattern similarity across different cues were gradually reduced (Fig. 7), implying an increasingly pronounced pattern separation. This finding is in line with recent research illustrating robust pattern separation over time during the learning process.[21] Beyond the left hippocampus, we identified the most robust pattern separation in the left medial frontal region,[49] underscoring the significance of the vmPFC in episodic memory.[50] This vmPFC-hippocampus network finding echoes previous research in pattern separation,[51] prospective memory[52] and concept construction.[53] Interestingly, we observed that the pattern separation persisted even after the shifting to the memory retrieval strategy. This is consistent with our model's prediction that trials after strategy transition still undergo memory strength enhancement (Fig. S1A).

In conclusion, the present study demonstrates that practice is accompanied by a transition from rule-based to memory-based strategy to improve performance and reduce effort. This transition can be accounted for by a computational model with cost-benefit tradeoff between strategies. Model-based fMRI analysis revealed different encoding of strength and content, with the former relying on different regions but the latter underlies widespread overlapping brain regions supporting both strategies by exhibiting strategy-specific activation patterns. Moreover, the transition is associated with neural representational change in the dlPFC and pattern separation in the vmPFC and hippocampus. These findings extend our understanding of how practice is associated with neural and behavioral changes in how tasks are represented and executed to improve performance.

Acknowledgement

This project was supported by the National Institute of Mental Health (R01MH131559 to J.J.). This work was conducted on an MRI instrument funded by S10RR028821. We thank Kai Hwang, Jan Wessel, Eliot Hazeltine, Atsushi Kikumoto, the members of the Cognitive Control Collaborative and the members of the Human Perception and Performance Group at the University of Iowa for helpful discussions.

Author Contributions

Conceptualization: J.J. and G.Y.; Data curation: G.Y.; Formal Analysis: J.J. and G.Y.; Funding acquisition: J.J.; Investigation: J.J. and G.Y.; Methodology: J.J. and G.Y.; Supervision: J.J.; Writing – original draft: G.Y.; Writing – review & editing: J.J. and G.Y.

Declaration of Interests

The authors declare no competing interests.

Materials and Methods

Subjects

We enrolled 36 participants. Two subjects were excluded due to lower than 70% accuracy in the test phase (see below). One more subject was excluded due to excessive head motion. The final sample consisted of 33 participants (18-42 years old, average of 25.0 ± 6.9 years; 22 females). All participants reported no history of psychiatric or neurological disorders, with normal or corrected-to-normal vision. The experiments were approved by the Institutional Review Board of the University of Iowa. Informed consent was obtained from all subjects prior to the experiment.

Experimental design

Training phase

Participants underwent online training to learn task transitions in sequences A (a→b→c→d→e) and B (d→c→a→e→b) (Fig. 4A). They performed multiple 5-trial mini-blocks to equip an avatar with gears based on a goal image (Fig. 1A). Each trial started with a sequence cue, succeeded by a goal image, a gear selection screen and feedback. To facilitate the learning of task transition, two test trials were administrated after each mini-block, in which participants indicated the 1st/2nd/3rd task following a cued task (Fig. S3). The training lasted 3-6 blocks and stopped when participants achieved a block-average accuracy of > 90% on test trials. Participants

underwent the above training between 4-24 hours before scanning and performed another short repetition (1-2 blocks) immediately before scanning. For a detailed description, see supplementary Note S3.

Test phase

The test phase was conducted in the scanner. The stimuli were back projected onto a screen (with a viewing angle of ~14.0° between the equipment pictures and the center of the screen) behind the subject and viewed via a surface mirror mounted onto the head coil. On each trial, a cue with a letter and a number indicating the sequence and position (e.g. A4) was shown at the center of the screen (Fig. 1B). Six equipment images, representing the five equipment types and a foil (MOUSTACHE), were shown around the cue. The images were randomly selected from the two images of each equipment type. The locations of the six equipment types were randomized at the subject level but fixed within each subject. Participants were asked to select the equipment type representing the cued task with a pair of button pads, each assigned with three fingers (index, middle and ring fingers). The screen proceeded to a fixation for 8s if participants responded correctly, or to feedback for 1s and then a fixation for 7s if an error was made or no response was received within 9s following the cue. The test phase consisted of 6 blocks of 40 trials each.

Behavioral analysis

The analysis was centered on test phase data with RT and ER as dependent variables. For RTs, we excluded the error trials (4.4%), and trials with outlier RTs (> 3 SDs above the median, 1.5%). We constructed an LME model, with the block (1–6), position (1–4, which enabled the isolation of the clean replay effect by excluding position 5—known to involve the recency effect[54]), their interaction and intercept as fixed effects. Each slope and the intercept also included a random effect at the subject level. We used the "AOCTOOL" and "multcompare" functions in Matlab to compare the slopes of position between different blocks. For all LME models conducted in this study, we estimated degree of freedoms with the Satterthwaite approach.[55] For the validation purpose, we expanded the analysis to include positions 1–5 (see supplementary Note S1).

Computational Model

We built a computational model to simulate how the brain chooses between replay and memory strategies using cost-benefit analysis. For cost, the replay strategy has a cost of replaying the sequence (C) compared to memory strategy. This cost is proportional to the number of steps replayed:

$$C = L_t - i, \quad (1)$$

where L_t is the cued position (e.g., 4 in cue A4), and i is the replay starting position. For example, when i is 1 and L_t is 4, the cost is 3 as the replay involves 3 steps (i.e., task transitions).

We operationalize the benefit as the probability of generating the correct response. For the replay strategy, as the participants have learned the transitions between steps from the training phase, the benefit depends on the strength of cue-task association at the starting position of the replay. For memory strategy, the benefit relies on the strength of cue-task association at the cued position. Thus, for each sequence we modeled the cue-task association using a probabilistic distribution for each position i on each trial t as $M_{i,t}(j)$, which represents the model's belief that the task j is at position i. At the beginning of the experiment (i.e., $t = 0$), $M_{i,t}(j)$ was initialized in the following manner: For position 1, we assumed a perfect memory from the training phase with a probability of 1 for the correct task. For positions 2–4, a uniform distribution was used to simulate the situation of no informative cue-task associations. In position 5, the probability of the correct task received a boost of γ to account for the recency effect; all other tasks had the same probability. After each trial, the probability distribution $M_{i,t}$ is updated as a result of learning the correct task at the cued position using a delta rule:

$$M_{i,t}(j) = \begin{cases} M_{i,t}(j)+\alpha*(1-M_{i,t}(j)), \text{ if } j \text{ is the true task at position } i \\ M_{i,t}(j) - \frac{\alpha*(1-M_{i,t}(j))}{4}, \text{ if } j \text{ is another task} \end{cases}, \quad (2)$$

where α is the learning rate ranging from 0 to 1.

The memory strength index S is quantified as the reversed entropy of $M_{i,t}$:

$$S = -H(M_{i,t}) = \sum_{j=1}^{5} p_j * \log(p_j) \quad (3)$$

Note that a higher S indicates a stronger memory strength. Therefore, the quantified value (i.e., cost-benefit tradeoff) for starting replay at position i is:

$$V_{i,t} = \lambda * S - C = -\lambda * H(M_{i,t}) - (L_t - i), \quad (4)$$

where λ is the tradeoff between cost and benefit, ranging from 0.01 to 100. On trial t the decision of choosing the best replay starting position i^* is determined by:

$$i^* = \underset{i}{\operatorname{argmax}}\,(V_{i,t}), \quad (5)$$

When i^* is the cued position, memory strategy is implemented as no replay is needed. When i^* is before the cued position, replay strategy is selected.

Model fitting

We hypothesized that the RT for the replay and memory trials would be influenced by the replay cost and memory strength, respectively. Therefore, we fit the model outputs to the RT using a linear regression, which serves as the connection of the model predictions and behavior:

$$RT \sim C*Type_R + S*Type_M + Type_R + Type_M + C*Times_R + \log(Trial) + Response, \quad (6)$$

where the $Type_R$ and $Type_M$ encode the factors of replay and memory trials, respectively, while the $C*Times_R$ encodes the interaction between replay cost and aggregated number of replayed steps since the beginning of experiment. Response is a categorical factor encoding the response buttons. The objective function was defined

as the residual sum of squares (RSS) from Eq. 6. To estimate the free parameters α, λ and γ, we ran the optimization 100 times (using fmincon in Matlab) with random starting values and chose the values led to the minimum RSS. To determine the best structure of the regression model, we compared this model to its reduced versions (Table 1) using likelihood ratio test. The likelihood of each alternative model was estimated using an LME model incorporating data and predictors from all subjects. P values comparing the unrestricted model (M0) to each of the restricted models (M1–M5) were obtained through the ratio of likelihood, assessed against a chi-square null distribution, with degrees of freedom equal to the difference in the number of parameters between the two models. Comparison between the alternative models were achieved using either likelihood ratio test when they are nested or Akaike information criterion (AIC) otherwise. P value for the AIC comparison was estimated with exp(–ΔAIC/2) between two models.

Behavioral transition point analysis

To estimate the group-level effect of post-strategy switch slowing,[22] we conducted an LME model using the trial type to predict RTs for the last replay and first memory trial. An intercept was added to capture the average RT. All predictors are treated as both the fixed effect and random effect at the subject level. Therefore, the model takes the following form:

$$RT = \beta_0 + \beta_1 TrialType + C + S + C*Times_R + \log(Trial) + RandomSlopes + \varepsilon, \quad (7)$$

where TrialType encodes either replay or memory trials, and RandomSlopes represents the random effect for the intercept and the slope of each fixed effect. We also estimated the null distribution for the post-strategy switch slowing by repeating the LME analysis using random permutation tests, in which transition points were shuffled for 5,000 times. To test if the model inherently introduces the post-strategy switch slowing, we ran an additional permutation test by randomizing the model parameters for 5,000 times. The p value was determined by the percentage of permutations inconsistent with the null hypothesis (e.g., with stronger or same post-switch slowing than the real data in this test).

fMRI Image acquisition and preprocessing

Functional imaging was performed on a 7T GE 950 scanner using echo-planar imaging (EPI) sensitive to BOLD contrast [in-plane resolution of 1.7 × 1.7 mm^2, 128 × 128 matrix, 75 slices with a thickness of 2.0 mm and no interslice skip, repetition time (TR) of 1000 ms, multiband acceleration factor of 4, echo-time (TE) of 20.5 ms, and a flip angle of 50°]. In addition, a sagittal T1-weighted anatomical image was acquired as a structural reference scan, with a total of 512 slices at a thickness of 0.43 mm with no gap and an in-plane resolution of 0.70 × 0.43 mm^2.

Before preprocessing, the first eight volumes of the functional images were removed due to the unstable signals. The anatomical and functional data were preprocessed with the fMRIprep 22.0.2[56] (RRID:SCR_016216), which is based on

Nipype 1.8.5[57] (RRID:SCR_002502). The BOLD time-series were resampled to the MNI152NLin2009cAsym space without smoothing. For a more detailed description of preprocessing, see supplementary Note S4. After preprocessing, we resampled the functional data to a spatial resolution of $2 \times 2 \times 2$ mm^3. The preprocessed data was smoothed with a full width at half maximum (FWHM) Gaussian kernel of 6 mm and 2mm for univariate and representational similarity analysis (RSA), respectively. All analyses were conducted in volumetric space, and surface maps are produced with Connectome Workbench (https://www.humanconnectome.org/software/connectome-workbench) for display purpose only.

Estimation of fMRI activation

A generalized linear model (GLM) was conducted across six sessions (one for each block), with each session comprising of trial-wise regressors time-locked to the onset of the cue. These regressors were convolved with a canonical hemodynamic response function (HRF) in SPM 12 (http://www.fil.ion.ucl.ac.uk/spm). We further added volume-level nuisance regressors, including the six head motion parameters, global signal, white matter signal, cerebrospinal fluid signal, and outlier TRs (defined as standard DVARS > 5 or frame-displacement > 0.9 mm from previous TR). Low-frequency signal drifts were filtered using a cutoff period of 128 s. The GLM yielded one beta map per trial, which was then noise normalized by dividing the original beta coefficients by the square root of the covariance matrix of the error terms.[58] The noise normalization was done separately for each of the 426 ROIs based on the extended Human Connectome Project multimodal parcellation atlas (HCPex, version 1.1[59]), resulting in one fMRI activation map for each trial. Error trials, outlier RT trials, and trials including large head movement volumes were excluded from further analysis. ROIs containing less than 50 voxels (i.e., 37 subcortical regions) were excluded from further analyses.

Univariate mixed-effect model analyses

We conducted two LME models to analyze the ROI-averaged fMRI activation. The first LME model was conducted on replay trials and incorporated several fixed effect regressors, including the replay cost C, $C*Times_R$, and the logarithm of trial number. The second LME model was conducted on memory trials and included fixed effect regressors of memory strength and the logarithm of trial number. Each model also included an intercept term. Additionally, the intercept and the slope of each regressor were also treated as random effects at the subject level. All predictors were z standardized. Statistical results were corrected for multiple comparisons across all the ROIs with false discovery rate (FDR) at the level of $q < 0.05$, with each individual ROI at uncorrected $p < .001$, both one-tailed for the replay trials and two-tailed for the memory trials based on our different hypotheses (see Results).

RSA

For each ROI, representational similarity between trials from different runs was defined as their voxel-wise correlation coefficient. Trial pairs from the same run were excluded due to their inflated similarity scores.[60,61] Vectorized representational similarity data were used as dependent variable in LME model analysis. In addition to fixed effects of interest, we added the intercept and two nuisance fixed effects encoding ROI-mean activation of each of the two trials to rule out the influence of activation strength on similarity score. Random effects consisted of the intercept and the slope for each fixed effect at the subject level. Statistical results were corrected for multiple comparisons across all the ROIs with FDR at the level of $q < 0.05$, with each individual ROI at uncorrected $p < 0.001$, both one-tailed. For the detailed LME models, see supplementary Note S5.

References

1. Fitts, P.M., and Posner, M.I. (1967). Human performance.
2. Anderson, J.R. (1982). Acquisition of cognitive skill. Psychological review *89*, 369-406. 10.1037/0033-295x.89.4.369.
3. Miller, E.K., and Cohen, J.D. (2001). An integrative theory of prefrontal cortex function. Annu Rev Neurosci *24*, 167-202. 10.1146/annurev.neuro.24.1.167.
4. Schneider, W., and Detweiler, M. (1988). A connectionist/control architecture for working memory. In Psychology of learning and motivation, (Elsevier), pp. 53-119.
5. Sheridan, H., and Reingold, E.M. (2017). Chess players' eye movements reveal rapid recognition of complex visual patterns: Evidence from a chess-related visual search task. J Vis *17*, 4. 10.1167/17.3.4.
6. van Opheusden, B., Kuperwajs, I., Galbiati, G., Bnaya, Z., Li, Y., and Ma, W.J. (2023). Expertise increases planning depth in human gameplay. Nature *618*, 1000-1005. 10.1038/s41586-023-06124-2.
7. Bilalic, M., Langner, R., Erb, M., and Grodd, W. (2010). Mechanisms and neural basis of object and pattern recognition: a study with chess experts. Journal of experimental psychology. General *139*, 728-742. 10.1037/a0020756.
8. Logan, G.D. (1988). Toward an instance theory of automatization. Psychological review *95*, 492-527. 10.1037/0033-295x.95.4.492.
9. Dolan, Ray J., and Dayan, P. (2013). Goals and Habits in the Brain. Neuron *80*, 312-325. 10.1016/j.neuron.2013.09.007.
10. Evans, J.S., and Stanovich, K.E. (2013). Dual-Process Theories of Higher Cognition: Advancing the Debate. Perspect Psychol Sci *8*, 223-241. 10.1177/1745691612460685.
11. Evans, J.S.B.T. (2008). Dual-Processing Accounts of Reasoning, Judgment, and Social Cognition. Annual review of psychology *59*, 255-278. 10.1146/annurev.psych.59.103006.093629.
12. Kahneman, D. (2011). Thinking, fast and slow (macmillan).
13. Shenhav, A., Botvinick, M.M., and Cohen, J.D. (2013). The expected value of control: an integrative theory of anterior cingulate cortex function. Neuron *79*, 217-240. 10.1016/j.neuron.2013.07.007.
14. Musslick, S., and Cohen, J.D. (2021). Rationalizing constraints on the capacity for cognitive control. Trends Cogn Sci *25*, 757-775. 10.1016/j.tics.2021.06.001.
15. Schuck, N.W., Gaschler, R., Wenke, D., Heinzle, J., Frensch, P.A., Haynes, J.D., and Reverberi, C. (2015). Medial prefrontal cortex predicts internally driven strategy shifts. Neuron *86*, 331-340. 10.1016/j.neuron.2015.03.015.
16. Baldassano, C., Chen, J., Zadbood, A., Pillow, J.W., Hasson, U., and Norman, K.A. (2017). Discovering event structure in continuous narrative perception and memory. Neuron *95*, 709-721. e705.
17. Clewett, D., DuBrow, S., and Davachi, L. (2019). Transcending time in the brain: How event memories are constructed from experience. Hippocampus *29*, 162-183. 10.1002/hipo.23074.

18. Silva, M., Baldassano, C., and Fuentemilla, L. (2019). Rapid Memory Reactivation at Movie Event Boundaries Promotes Episodic Encoding. J Neurosci *39*, 8538-8548. 10.1523/jneurosci.0360-19.2019.
19. Lohnas, L.J., Healey, M.K., and Davachi, L. (2023). Neural temporal context reinstatement of event structure during memory recall. Journal of experimental psychology. General *152*, 1840-1872. 10.1037/xge0001354.
20. Yassa, M.A., and Stark, C.E.L. (2011). Pattern separation in the hippocampus. Trends Neurosci *34*, 515-525. 10.1016/j.tins.2011.06.006.
21. Mill, R.D., and Cole, M.W. (2023). Neural representation dynamics reveal computational principles of cognitive task learning. bioRxiv. 10.1101/2023.06.27.546751.
22. Lemaire, P., and Lecacheur, M. (2010). Strategy switch costs in arithmetic problem solving. Mem Cognit *38*, 322-332. 10.3758/MC.38.3.322.
23. Jansma, J.M., Ramsey, N.F., Coppola, R., and Kahn, R.S. (2000). Specific versus nonspecific brain activity in a parametric N-back task. Neuroimage *12*, 688-697. 10.1006/nimg.2000.0645.
24. Brodt, S., Pöhlchen, D., Flanagin, V.L., Glasauer, S., Gais, S., and Schönauer, M. (2016). Rapid and independent memory formation in the parietal cortex. Proceedings of the National Academy of Sciences *113*, 13251-13256. 10.1073/pnas.1605719113.
25. Critchley, H.D., Mathias, C.J., and Dolan, R.J. (2001). Neural activity in the human brain relating to uncertainty and arousal during anticipation. Neuron *29*, 537-545. 10.1016/s0896-6273(01)00225-2.
26. Glasser, M.F., Coalson, T.S., Robinson, E.C., Hacker, C.D., Harwell, J., Yacoub, E., Ugurbil, K., Andersson, J., Beckmann, C.F., Jenkinson, M., et al. (2016). A multi-modal parcellation of human cerebral cortex. Nature *536*, 171-178. 10.1038/nature18933.
27. Knutson, K.M., Wood, J.N., and Grafman, J. (2004). Brain activation in processing temporal sequence: an fMRI study. Neuroimage *23*, 1299-1307. 10.1016/j.neuroimage.2004.08.012.
28. Wagner, A.D., Shannon, B.J., Kahn, I., and Buckner, R.L. (2005). Parietal lobe contributions to episodic memory retrieval. Trends Cogn Sci *9*, 445-453. 10.1016/j.tics.2005.07.001.
29. Squire, L.R., Stark, C.E., and Clark, R.E. (2004). The medial temporal lobe. Annu Rev Neurosci *27*, 279-306. 10.1146/annurev.neuro.27.070203.144130.
30. Olafsdottir, H.F., Bush, D., and Barry, C. (2018). The Role of Hippocampal Replay in Memory and Planning. Curr Biol *28*, R37-R50. 10.1016/j.cub.2017.10.073.
31. Radvansky, G.A., and Zacks, J.M. (2017). Event Boundaries in Memory and Cognition. Curr Opin Behav Sci *17*, 133-140. 10.1016/j.cobeha.2017.08.006.
32. Lieder, F., and Griffiths, T.L. (2017). Strategy selection as rational metareasoning. Psychological review *124*, 762-794. 10.1037/rev0000075.

33. Shenhav, A., Musslick, S., Lieder, F., Kool, W., Griffiths, T.L., Cohen, J.D., and Botvinick, M.M. (2017). Toward a Rational and Mechanistic Account of Mental Effort. Annu Rev Neurosci *40*, 99-124. 10.1146/annurev-neuro-072116-031526.
34. Jiang, J., Beck, J., Heller, K., and Egner, T. (2015). An insula-frontostriatal network mediates flexible cognitive control by adaptively predicting changing control demands. Nat Commun *6*, 8165. 10.1038/ncomms9165.
35. Collins, A., and Koechlin, E. (2012). Reasoning, Learning, and Creativity: Frontal Lobe Function and Human Decision-Making. PLOS Biology *10*, e1001293. 10.1371/journal.pbio.1001293.
36. McDougle, S.D., and Taylor, J.A. (2019). Dissociable cognitive strategies for sensorimotor learning. Nat Commun *10*, 40. 10.1038/s41467-018-07941-0.
37. Curtis, C.E., and D'Esposito, M. (2003). Persistent activity in the prefrontal cortex during working memory. Trends Cogn Sci *7*, 415-423. 10.1016/s1364-6613(03)00197-9.
38. Xie, Y., Hu, P., Li, J., Chen, J., Song, W., Wang, X.J., Yang, T., Dehaene, S., Tang, S., Min, B., and Wang, L. (2022). Geometry of sequence working memory in macaque prefrontal cortex. Science *375*, 632-639. 10.1126/science.abm0204.
39. Kuhl, B.A., and Chun, M.M.J.J.o.N. (2014). Successful remembering elicits event-specific activity patterns in lateral parietal cortex. *34*, 8051-8060.
40. Buckner, R.L., Koutstaal, W., Schacter, D.L., Wagner, A.D., and Rosen, B.R. (1998). Functional-anatomic study of episodic retrieval using fMRI. I. Retrieval effort versus retrieval success. Neuroimage *7*, 151-162. 10.1006/nimg.1998.0327.
41. Lewis-Peacock, J.A., Drysdale, A.T., and Postle, B.R. (2015). Neural Evidence for the Flexible Control of Mental Representations. Cerebral cortex (New York, N.Y. : 1991) *25*, 3303-3313. 10.1093/cercor/bhu130.
42. Duncan, J. (2001). An adaptive coding model of neural function in prefrontal cortex. Nat Rev Neurosci *2*, 820-829. 10.1038/35097575.
43. Duncan, J. (2013). The structure of cognition: attentional episodes in mind and brain. Neuron *80*, 35-50. 10.1016/j.neuron.2013.09.015.
44. Kuhl, B.A., Dudukovic, N.M., Kahn, I., and Wagner, A.D. (2007). Decreased demands on cognitive control reveal the neural processing benefits of forgetting. Nature neuroscience *10*, 908-914. 10.1038/nn1918.
45. Kuhl, B.A., Shah, A.T., DuBrow, S., and Wagner, A.D. (2010). Resistance to forgetting associated with hippocampus-mediated reactivation during new learning. Nature neuroscience *13*, 501-506. 10.1038/nn.2498.
46. Davis, T., LaRocque, K.F., Mumford, J.A., Norman, K.A., Wagner, A.D., and Poldrack, R.A.J.N. (2014). What do differences between multi-voxel and univariate analysis mean? How subject-, voxel-, and trial-level variance impact fMRI analysis. *97*, 271-283.
47. Jimura, K., and Poldrack, R.A.J.N. (2012). Analyses of regional-average activation and multivoxel pattern information tell complementary stories. *50*, 544-552.

48. Wanjia, G., Favila, S.E., Kim, G., Molitor, R.J., and Kuhl, B.A. (2021). Abrupt hippocampal remapping signals resolution of memory interference. Nat Commun *12*, 4816. 10.1038/s41467-021-25126-0.
49. Nash, M.I., Hodges, C.B., Muncy, N.M., and Kirwan, C.B. (2021). Pattern separation beyond the hippocampus: A high-resolution whole-brain investigation of mnemonic discrimination in healthy adults. Hippocampus *31*, 408-421. 10.1002/hipo.23299.
50. Euston, D.R., Gruber, A.J., and McNaughton, B.L. (2012). The role of medial prefrontal cortex in memory and decision making. Neuron *76*, 1057-1070. 10.1016/j.neuron.2012.12.002.
51. Guise, K.G., and Shapiro, M.L. (2017). Medial Prefrontal Cortex Reduces Memory Interference by Modifying Hippocampal Encoding. Neuron *94*, 183-192 e188. 10.1016/j.neuron.2017.03.011.
52. Brown, T.I., Carr, V.A., LaRocque, K.F., Favila, S.E., Gordon, A.M., Bowles, B., Bailenson, J.N., and Wagner, A.D. (2016). Prospective representation of navigational goals in the human hippocampus. Science *352*, 1323-1326. 10.1126/science.aaf0784.
53. Bowman, C.R., and Zeithamova, D. (2018). Abstract Memory Representations in the Ventromedial Prefrontal Cortex and Hippocampus Support Concept Generalization. J Neurosci *38*, 2605-2614. 10.1523/jneurosci.2811-17.2018.
54. Talmi, D., and Goshen-Gottstein, Y.J.M. (2006). The long-term recency effect in recognition memory. *14*, 424-436.
55. Satterthwaite, F.E. (1946). An Approximate Distribution of Estimates of Variance Components. Biometrics Bulletin *2*. 10.2307/3002019.
56. Esteban, O., Markiewicz, C.J., Blair, R.W., Moodie, C.A., Isik, A.I., Erramuzpe, A., Kent, J.D., Goncalves, M., DuPre, E., Snyder, M., et al. (2019). fMRIPrep: a robust preprocessing pipeline for functional MRI. Nat Methods *16*, 111-+. 10.1038/s41592-018-0235-4.
57. Gorgolewski, K., Burns, C.D., Madison, C., Clark, D., Halchenko, Y.O., Waskom, M.L., and Ghosh, S.S. (2011). Nipype: a flexible, lightweight and extensible neuroimaging data processing framework in python. Frontiers in neuroinformatics *5*, 13. 10.3389/fninf.2011.00013.
58. Walther, A., Nili, H., Ejaz, N., Alink, A., Kriegeskorte, N., and Diedrichsen, J. (2016). Reliability of dissimilarity measures for multi-voxel pattern analysis. Neuroimage *137*, 188-200. 10.1016/j.neuroimage.2015.12.012.
59. Huang, C.C., Rolls, E.T., Feng, J., and Lin, C.P. (2022). An extended Human Connectome Project multimodal parcellation atlas of the human cortex and subcortical areas. Brain Struct Funct *227*, 763-778. 10.1007/s00429-021-02421-6.
60. Cai, M.B., Schuck, N.W., Pillow, J.W., and Niv, Y. (2019). Representational structure or task structure? Bias in neural representational similarity analysis and a Bayesian method for reducing bias. PLoS Comput Biol *15*, e1006299. 10.1371/journal.pcbi.1006299.

61. Mumford, J.A., Davis, T., and Poldrack, R.A. (2014). The impact of study design on pattern estimation for single-trial multivariate pattern analysis. Neuroimage *103*, 130-138. 10.1016/j.neuroimage.2014.09.026.